PSFC/RR-02-5

A Quasi-2D Model for Helium Flow in Two-Channel CICC

Jun Feng

September 13, 2002

Plasma Science and Fusion Center
Massachusetts Institute of Technology
Cambridge, MA 02139, USA

This work was supported by the US Department of Energy, Grant No. DE-FC02-93ER54186.

Table of Contents

Abstract

A quasi-2D model for two channel helium flow in CICC has been developed. This model is derived from fundamental thermohydraulic equations, and implicitly analyzes the mass, moment and energy exchange between two channels. The helium flow rates between two channels are treated as independent variables, and are solved in parallel with other independent variables such as pressures, temperatures and velocities. This new model may provide more in-depth understanding of thermohydraulic performance of helium flow in two channel superconducting coils.

1. Introduction

CSMC and CSIC are all made of two-channel superconductor cables. Therefore, a sophisticated two-channel model becomes necessary for simulating thermohydraulic and quenching behavior of the CSMC/CSIC.

Several researchers [1,2,3] have analyzed this problem in detail. Bottura[1] developed a one dimensional model, in which he assumed that the helium temperature and pressure in both bundle and central hole are the same. Bottura's model also sets helium pressure as one of the independent variables, and therefore all codes based on his model show excellent stability even as the pressure different between inlet and outlet is very small. However, Bottura's 1D model neglects the mass, moment and energy exchange between the two channels. The effect of such simplification on all over results is unknown.

Zanino et al.[2] further developed Bottura's 1D model by incorporating mass, moment and energy exchange between two channels into his new 1D model. He simply assumed that the helium flow rate $v_\perp$ between two channels is proportional to the square root of pressure difference dp between two channels:

$$v_\perp = \sqrt{\frac{2|dp|}{kr}}\frac{dp}{|dp|}\ , \qquad (1.1)$$

where: k is loss coefficient due to flow resistance between two channels. This assumption was then applied to explicitly define, in Buttura's 1D model, all extra terms which represent the mass, moment and energy exchanges between two channels. Equation 1.1 is based on Bernoulli equation in static flow, and without considering any dynamic variables. The effect of such simplification may need further exploration.

A new model for two channel helium flow in CICC has been developed, and reported below. This model is derived from fundamental thermohydraulic equations, and implicitly analyzes the mass, moment and energy exchange between two channels. The helium flow rates between two channels are treated as independent variables, and are solved in parallel with other independent variables such as pressures, temperatures and velocities. This new model may provide more in-depth understanding of thermohydraulic performance of helium flow in two channel superconducting coils.

The following sections will first discuss a set of general thermohydraulic equations, which are then applied to CICC for a 2D thermohydraulic model. Finally, the approach of a quasi-2D model to use 1D method for solution of a 2D problem will be reported.

2. Development of a 2D model for two-channel helium flow in CICC

As further development of Bottura's 1D formulations,[1] the following derivations lead to a set of corresponding 3D formulations, which are then applied for the 2D application in two-channel helium flow.

2.1 Derivation of a pressure-based energy balance equation

The general governing equations of mass, momentum and energy balance for helium flow in CICC are respectively:[4]

$$\frac{\partial r}{\partial t} + \nabla \cdot (r\vec{v}) = 0 , \tag{2.1.1}$$

$$\frac{\partial}{\partial t}(r\vec{v}) + \nabla \cdot r\vec{v}\vec{v} = -\nabla p - r\vec{F} , \tag{2.1.2}$$

$$\frac{\partial}{\partial t}(re) + \nabla \cdot (re + p)\vec{v} = \frac{Q}{A} , \tag{2.1.3}$$

where: the viscosity effects are neglected, and the friction force is defined as

$$\vec{F} = 2 f \frac{\vec{v}|\vec{v}|}{D_h} . \tag{2.1.4}$$

The total specific energy e and specific enthalpy h are defined respectively as

$$e = i + \frac{v^2}{2} , \tag{2.1.5}$$

and

$$h = i + \frac{p}{r} , \tag{2.1.6}$$

where: i is the specific internal energy.

The momentum balance equation 2.1.2 can be expressed alternatively as:

$$r \frac{\partial \vec{v}}{\partial t} + (r\vec{v} \cdot \nabla)\vec{v} = -\nabla p - r\vec{F} . \tag{2.1.7}$$

Substituting Eqs. 2.1.5 and 2.1.6 into Eq. 2.1.3 gives

$$\frac{\partial}{\partial t}\left(rh - p + r\frac{v^2}{2} \right) + \nabla \cdot \left(hr\vec{v} + \frac{v^2}{2} r\vec{v} \right) = \frac{Q}{A} \ . \tag{2.1.8}$$

Further expanding Eq. 2.1.8 results in:

$$\frac{\partial}{\partial t}(rh) - \frac{\partial p}{\partial t} + \frac{\partial}{\partial t}\left(r\frac{\vec{v}\cdot\vec{v}}{2} \right) + \nabla \cdot (hr\vec{v}) + \nabla \cdot \left(\frac{\vec{v}\cdot\vec{v}}{2} r\vec{v} \right) = \frac{Q}{A} \ . \tag{2.1.9}$$

By applying the following rules of vector operator:[5]

$$\nabla \cdot (hr\vec{v}) = h\nabla \cdot (r\vec{v}) + r\vec{v} \cdot \nabla h \tag{2.1.10}$$

and

$$\nabla \cdot \left(\frac{\vec{v}\cdot\vec{v}}{2} r\vec{v} \right) = \frac{\vec{v}\cdot\vec{v}}{2} \nabla \cdot (r\vec{v}) + r\vec{v} \cdot \nabla \frac{\vec{v}\cdot\vec{v}}{2}, \tag{2.1.11}$$

Eq. 2.1.9 becomes

$$r\frac{\partial h}{\partial t} + r\vec{v} \cdot \nabla h + h\left(\frac{\partial r}{\partial t} + \nabla \cdot (r\vec{v}) \right) - \frac{\partial p}{\partial t} + r\frac{\partial}{\partial t}\left(\frac{\vec{v}\cdot\vec{v}}{2} \right) + r\vec{v} \cdot \nabla \frac{\vec{v}\cdot\vec{v}}{2} + \frac{\vec{v}\cdot\vec{v}}{2}\left(\frac{\partial r}{\partial t} + \nabla \cdot (r\vec{v}) \right) = \frac{Q}{A}. \tag{2.1.12}$$

Applying mass balance equation 2.1.1 reduces Eq. 2.1.12 to

$$r\frac{\partial h}{\partial t} + r\vec{v} \cdot \nabla h - \frac{\partial p}{\partial t} + r\vec{v} \cdot \frac{\partial \vec{v}}{\partial t} + r\vec{v} \cdot \nabla \frac{\vec{v}\cdot\vec{v}}{2} = \frac{Q}{A} \ . \tag{2.1.13}$$

The 1st and 2nd terms of the left side of Eq. 2.1.13 involve the enthalpy, which is related to pressure and density by the following thermodynamics relation:[1]

$$dr = \frac{1+j}{c^2} dp - \frac{rf}{c^2} dh. \tag{2.1.14}$$

where: c is the isotropic speed of sound in helium, and f is the Gruneisen parameter,

$$f = \left(\frac{r}{T}\frac{\partial T}{\partial r} \right)_S . \tag{2.1.15}$$

Manipulation of Eq. 2.1.14 leads to:

$$r f \frac{\partial h}{\partial t} = (1+f)\frac{\partial p}{\partial t} - c^2 \frac{\partial r}{\partial t}, \tag{2.1.16}$$

and

$$r f \nabla h = (1+f)\nabla p - c^2 \nabla r \ . \tag{2.1.17}$$

Let's examine the 4th and 5th terms involving kinetic energy in the left side of Eq. 2.1.13. The following rules of vector operator are applied:[5]

$$\nabla \frac{\vec{v}\cdot\vec{v}}{2} = \vec{v}\times\nabla\times\vec{v} + (\vec{v}\cdot\nabla)\vec{v}\,, \tag{2.1.18}$$

and

$$\vec{v}\cdot\vec{v}\times\nabla\times\vec{v} = 0\,. \tag{2.1.19}$$

The sum of the 4th and 5th terms then becomes:

$$r\vec{v}\cdot\frac{\partial\vec{v}}{\partial t} + r\vec{v}\cdot\nabla\frac{\vec{v}\cdot\vec{v}}{2} = \vec{v}\cdot\left(r\frac{\partial\vec{v}}{\partial t} + (r\vec{v}\cdot\nabla)\vec{v}\right). \tag{2.1.20}$$

Substituting momentum balance equation 2.1.7 into Eq. 2.1.20 gives

$$r\vec{v}\cdot\frac{\partial\vec{v}}{\partial t} + r\vec{v}\cdot\nabla\frac{\vec{v}\cdot\vec{v}}{2} = -\vec{v}\cdot\nabla p - r\vec{v}\cdot\vec{F}\,. \tag{2.1.21}$$

The 1st, 2nd, 4th, and 5th terms of Eq. 2.1.13 are replaced with new expressions in 2.1.16, 2.1.17 and 2.1.21, and Eq. 2.1.13 becomes

$$\frac{1}{f}\frac{\partial p}{\partial t} - \frac{c^2}{f}\left(\frac{\partial r}{\partial t} + \vec{v}\cdot\nabla r\right) + \frac{1}{f}\vec{v}\cdot\nabla p - r\vec{v}\cdot\vec{F} = \frac{Q}{A}. \tag{2.1.22}$$

Applying mass balance Eq. 2.1.1 in Eq. 2.1.22, we then have the final form of the general pressure-based energy balance equation as:

$$\frac{\partial p}{\partial t} + v\cdot\nabla p + rc^2\nabla\cdot\vec{v} = f\left(\frac{Q}{A} + r\vec{v}\cdot\vec{F}\right). \tag{2.1.23}$$

Eq. 2.1.23 can be reduced to Bottura's 1D equation[1] for 1D modeling as:

$$\frac{\partial p}{\partial t} + v_x\frac{\partial p}{\partial x} + rc^2\frac{\partial v_x}{\partial x} = f\left(\frac{Q}{A} + rv_xF_x\right). \tag{2.1.24}$$

2.2 Derivation of a temperature-based energy balance equation

Again, start from the general energy balance equation 2.1.3:

$$\frac{\partial}{\partial t}(re)+\nabla\cdot(re+p)\vec{v}=\frac{Q}{A}. \qquad (2.1.3)$$

Substituting Eq. 2.1.5: $e=i+\frac{v^2}{2}$ into Eq. 2.1.3 gives

$$\frac{\partial}{\partial t}(ri)+\frac{\partial}{\partial t}\left(r\frac{v^2}{2}\right)+\nabla\cdot(ir\vec{v})+\nabla\cdot\left(\frac{v^2}{2}r\vec{v}\right)+\nabla\cdot(p\vec{v})=\frac{Q}{A}. \qquad (2.2.1)$$

Manipulation of Eq. 2.2.1 and using vector operators as same as in the last section result in:

$$r\frac{\partial i}{\partial t}+r\vec{v}\cdot\nabla i+i\left(\frac{\partial r}{\partial t}+\nabla\cdot(r\vec{v})\right)+r\frac{\partial}{\partial t}\left(\frac{\vec{v}\cdot\vec{v}}{2}\right)+r\vec{v}\cdot\nabla\left(\frac{\vec{v}\cdot\vec{v}}{2}\right)+\frac{\vec{v}\cdot\vec{v}}{2}\left(\frac{\partial r}{\partial t}+\nabla\cdot(r\vec{v})\right)+\nabla\cdot(p\vec{v})=\frac{Q}{A}. \qquad (2.2.2)$$

Applying mass balance equation 2.1.1 reduces Eq. 2.2.2 to

$$r\frac{\partial i}{\partial t}+r\vec{v}\cdot\nabla i+r\vec{v}\cdot\frac{\partial\vec{v}}{\partial t}+r\vec{v}\cdot\nabla\left(\frac{\vec{v}\cdot\vec{v}}{2}\right)+\nabla\cdot(p\vec{v})=\frac{Q}{A}. \qquad (2.2.3)$$

The 1st and 2nd terms of the left side in Eq. 2.2.3 involve specific internal energy i, which can be related to density and temperature by the following thermodynamics relation:[1]

$$di=\left(\frac{p}{r}-fC_vT\right)\frac{dr}{r}+C_v dT, \qquad (2.2.4)$$

where: C_v is the specific heat at constant volume.

Eq. 2.2.4 can be expressed alternatively by:

$$r\frac{\partial i}{\partial t}=\left(\frac{p}{r}-fC_vT\right)\frac{\partial r}{\partial t}+rC_v\frac{\partial T}{\partial t}, \qquad (2.2.5)$$

and

$$r\nabla i=\left(\frac{p}{r}-fC_vT\right)\nabla r+rC_v\nabla T. \qquad (2.2.6)$$

The 3rd, 4th and 5th terms of the left side in Eq. 2.2.3 involve kinetic energy and work done by pressure. Again using vector operators and momentum balance equation 2.1.7, we have:

$$r\vec{v}\cdot\frac{\partial\vec{v}}{\partial t}+r\vec{v}\cdot\nabla\left(\frac{\vec{v}\cdot\vec{v}}{2}\right)+\nabla\cdot\left(p\vec{v}\right)=p\nabla\cdot\vec{v}-r\vec{v}\cdot\vec{F}\ . \tag{2.2.7}$$

Substituting Eqs. 2.2.5, 2.2.6 and 2.2.7 into Eq. 2.2.3 gives

$$\left(\frac{p}{r}-fC_vT\right)\frac{\partial r}{\partial t}+rC_v\frac{\partial T}{\partial t}+\left(\frac{p}{r}-fC_vT\right)\vec{v}\cdot\nabla r+rC_v\vec{v}\cdot\nabla T+p\nabla\cdot\vec{v}=\frac{Q}{A}+r\vec{v}\cdot\vec{F}\ . \tag{2.2.8}$$

Appling mass balance equation 2.1.1 reduces Eq. 2.2.8 to the final form of the general temperature-based energy balance equation:

$$\frac{\partial T}{\partial t}+fT\nabla\cdot\vec{v}+\vec{v}\cdot\nabla T=\frac{1}{rC_v}\left(\frac{Q}{A}+r\vec{v}\cdot\vec{F}\right). \tag{2.2.9}$$

Eq. 2.2.9 can be reduced to Bottura's 1D equation[1] for 1D modeling as:

$$\frac{\partial T}{\partial t}+fT\frac{\partial v_x}{\partial x}+v_x\frac{\partial T}{\partial x}=\frac{1}{rC_v}\left(\frac{Q}{A}+rv_xF_x\right). \tag{2.2.10}$$

In summary, a set of general equations for 3D thermo hydraulic analysis of helium flow in CICC is listed as the following:

$$\frac{\partial r}{\partial t}+\nabla\cdot\left(r\vec{v}\right)=0\ , \tag{2.1.1}$$

$$r\frac{\partial\vec{v}}{\partial t}+\left(r\vec{v}\cdot\nabla\right)\vec{v}=-\nabla p-r\vec{F}\ , \tag{2.1.7}$$

$$\frac{\partial p}{\partial t}+\vec{v}\cdot\nabla p+rc^2\nabla\cdot\vec{v}=f\left(\frac{Q}{A}+r\vec{v}\cdot\vec{F}\right), \tag{2.1.23}$$

$$\frac{\partial T}{\partial t}+\vec{v}\cdot\nabla T+fT\nabla\cdot\vec{v}=\frac{1}{rC_v}\left(\frac{Q}{A}+r\vec{v}\cdot\vec{F}\right). \tag{2.2.9}$$

2.3 A 2D model for two-channel helium flow

Applying the general equations listed in the last section for 2D application gives a set of mass, momentum and energy balance equations for 2D helium flow in two-channel CICC:

$$\frac{\partial r}{\partial t} + r\left(\frac{\partial v_x}{\partial x} + \frac{1}{r}\frac{\partial}{\partial r}(rv_r)\right) + \left(v_x \frac{\partial r}{\partial x} + v_r \frac{\partial r}{\partial r}\right) = 0\,, \tag{2.3.1}$$

$$\frac{\partial v_x}{\partial t} + v_x \frac{\partial v_x}{\partial x} + v_r \frac{\partial v_x}{\partial r} = -\frac{1}{r}\frac{\partial p}{\partial x} - F_x\,, \tag{2.3.2}$$

$$\frac{\partial v_r}{\partial t} + v_x \frac{\partial v_r}{\partial x} + v_r \frac{\partial v_r}{\partial r} = -\frac{1}{r}\frac{\partial p}{\partial r} - F_r\,, \tag{2.3.3}$$

$$\frac{\partial p}{\partial t} + v_x \frac{\partial p}{\partial x} + v_r \frac{\partial p}{\partial r} + rc^2\left(\frac{\partial v_x}{\partial x} + \frac{1}{r}\frac{\partial}{\partial r}(rv_r)\right) = f\left(\frac{Q}{A} + rv_x F_x + rv_r F_r\right), \tag{2.3.4}$$

$$\frac{\partial T}{\partial t} + v_x \frac{\partial T}{\partial x} + v_r \frac{\partial T}{\partial r} + fT\left(\frac{\partial v_x}{\partial x} + \frac{1}{r}\frac{\partial}{\partial r}(rv_r)\right) = \frac{1}{rC_v}\left(\frac{Q}{A} + rv_x F_x + rv_r F_r\right). \tag{2.3.5}$$

3. Development of a quasi-2D model for two-channel helium flow in CICC

Solving the above equations Eqs. 2.3.1 to 2.3.5 will give accurate results for a 2D helium flow of CICC. However, the CPU time may be expensive for a 2D/3D code. Therefore, a quasi-2D model using 1D method to solve a 2D problem has been developed, and will be reported below.

3.1 Model assumptions

a. Since the axial dimension is much greater than the radial direction in the two-channel CICC, it is reasonable to assume that the pressure, temperature, density and axial velocity in each channel (i.e., bundle and central hole) are only functions of axial coordinates x;

b. The radial velocities in both channels only exist around the interface between 2 channels with effective distance in the order of the spring thickness. Other reasonable distribution functions of the radial velocities could be assumed (e.g., linear or exponential decrease from the interface etc.), but these different distribution functions only affect the radial momentum balance , and the preliminary analyses show that their effect on final results is very small.

3.2 Quasi-2D mass balance equations

The mass balance is controlled by Eq. 2.3.1. Integration of Eq. 2.3.1 over radial and angle coordinates can be performed by:

$$\iint (Eq.2.3.1)\,e\,r\,dr\,df \Rightarrow \int_0^{2p} df \int_0^{r_H} (Eq.2.3.1)\,e_H\,r\,dr + \int_0^{2p} df \int_{r_H}^{r_B} (Eq.2.3.1)\,e_B\,r\,dr\,, \tag{3.2.1}$$

where: r_B and r_H are the outside radius of the bundle annulus and central hole respectively. e_B and e_H are the percentage of helium space in the bundle and hole respectively. Apparently, in the current CICC cable design:

$$e_B = \frac{A_B}{p\left(r_B^2 - r_H^2\right)} \quad \text{and} \quad e_H = 1. \tag{3.2.2}$$

Implementation of Eq. 3.2.1 results in

$$A_B \frac{\partial r_B}{\partial t} + A_H \frac{\partial r_H}{\partial t} + A_B v_B \frac{\partial r_B}{\partial x} + A_H v_H \frac{\partial r_H}{\partial x} + A_B r_B \frac{\partial v_B}{\partial x} + A_H r_H \frac{\partial v_H}{\partial x}$$

$$+ 2pr_H\left(r_H v_{rH} - e_B r_B v_{rB}\right) = 0\ , \tag{3.2.3}$$

where: v_{rB} and v_{rH} are the radial velocities of helium in the bundle and hole respectively.

To replace density with pressure and temperature, by using the state equation

$$r = r(p,T)\ , \tag{3.2.4}$$

Eq. 3.2.3 can be converted into

$$A_B \frac{\partial r_B}{\partial p_B}\frac{\partial p_B}{\partial t} + A_B \frac{\partial r_B}{\partial T_B}\frac{\partial T_B}{\partial t} + A_H \frac{\partial r_H}{\partial p_H}\frac{\partial p_H}{\partial t} + A_H \frac{\partial r_H}{\partial T_H}\frac{\partial T_H}{\partial t}$$

$$+ A_B v_B \frac{\partial r_B}{\partial p_B}\frac{\partial p_B}{\partial x} + A_B v_B \frac{\partial r_B}{\partial T_B}\frac{\partial T_B}{\partial x} + A_H v_H \frac{\partial r_H}{\partial p_H}\frac{\partial p_H}{\partial x} + A_H v_H \frac{\partial r_H}{\partial T_H}\frac{\partial T_H}{\partial x}$$

$$+ A_B r_B \frac{\partial v_B}{\partial x} + A_H r_H \frac{\partial v_H}{\partial x} + 2pr_H\left(r_H v_{rH} - e_B r_B v_{rB}\right) = 0\,. \tag{3.2.5}$$

For first order approximation, assume that mass balance is established at the interface between the two channels, Eq. 3.2.5 can be simplified as:

$$r_H v_{rH} = e_B r_B v_{rB}\,. \tag{3.2.6}$$

3.3 Quasi-2D momentum balance equations

The momentum balance along x axis is controlled by Eq. 2.3.2 for both channels. Integration of Eq. 2.3.2 over radial and angle coordinates for each channel gives

$$\frac{\partial v_B}{\partial t} + v_B \frac{\partial v_B}{\partial x} = -\frac{1}{r_B}\frac{\partial p_B}{\partial x} - F_B \ , \tag{3.3.1}$$

and

$$\frac{\partial v_H}{\partial t} + v_H \frac{\partial v_H}{\partial x} = -\frac{1}{r_H}\frac{\partial p_H}{\partial x} - F_H \ . \tag{3.3.2}$$

The friction forces F_B and F_H are defined respectively for bundle and hole as:

$$F_B = 2 f_B \frac{v_B |v_B|}{D_{hB}}, \tag{3.3.3}$$

and

$$F_H = 2 f_H \frac{v_H |v_H|}{D_{hH}}, \tag{3.3.4}$$

where: f_B, f_H and D_{hB}, D_{hH} are friction factors and hydraulic diameters for the bundle and hole respectively.

The momentum balance along the radial direction is controlled by Eq. 2.3.3. Integration of Eq. 2.3.3 over radial and angle coordinates can be performed by

$$\iint (Eq.2.3.3) dr df \Rightarrow \int_0^{2p} df \int_0^{r_B} (Eq.2.3.3) dr \, . \tag{3.3.5}$$

Note that, by assumption, the helium radial velocities v_{rB} and v_{rH} only exist around the interface between the two channels over effective distances dr_{pB} and dr_{pH} for bundle and hole respectively. dr_{pB} and dr_{pH} are actually determined by the effective distance of the pressure difference between the two channels, and should be in the same order of the spring thickness. Implementation of the above integration gives

$$r_B dr_{pB} \frac{\partial v_{rB}}{\partial t} + r_H dr_{pH} \frac{\partial v_{rH}}{\partial t} + r_B dr_{pB} v_B \frac{\partial v_{rB}}{\partial x} + r_H dr_{pH} v_H \frac{\partial v_{rH}}{\partial x}$$

$$+ \left(r_H \frac{v_{rH}^2}{2} - r_B \frac{v_{rB}^2}{2} \right) = (p_H - p_B) - \overline{r} dr_f F_r \ . \tag{3.3.6}$$

The last term of Eq. 3.3.6 represents the radial interface resistance as helium flows from one channel to another. It is expressed in a form of friction force here. $\bar{r}$, dr_f and F_r are helium density at the interface, effective friction distance, and radial friction force respectively. $\bar{r}$ is about the average helium density of the two channels. dr_f is in the order of the spring thickness. F_r can be expressed as the same form as in Eq. 2.1.4 as:

$$F_r = 2 f_r \frac{v_r |v_r|}{D_{hr}}, \tag{3.3.7}$$

where: the radial hydraulic diameter D_{hr} is approximately twice the gap between turns of the spring. If the spring gap is zero (i.e., the interface is sealed), the radial interface resistance becomes infinite, and the radial helium flow reduces to zero. For coding simplicity, this term can be approximately written as:

$$\bar{r} dr_f F = k(p_H - p_B), \tag{3.3.8}$$

where: k is defined as the flow resistance coefficient at interface, and ranges from 0 to 1. $k = 1$ if the interface is sealed, and the radial helium flow reduces to zero. $k = 0$ if there is no flow resistance. In current CICC design, the interfacial spring is open up, and the radial flow velocity v_r is very small (in order of 10^{-6} m/s), we assume a zero flow resistance, i.e. $k = 0$.

3.4 Quasi-2D energy balance equations

The energy balance is controlled by Eqs. 2.3.4 and 2.3.5 for both channels. Integration of Eq. 2.3.4 over radial and angle coordinates for each of bundle and hole channel gives

$$\frac{\partial p_B}{\partial t} + v_B \frac{\partial p_B}{\partial x} + r_B c_B^2 \frac{\partial v_B}{\partial x} - \frac{2 r_H}{r_B^2 - r_H^2} r_B c_B^2 v_{rB} = f_B \left(\frac{Q_B}{A_B} + r_B v_B F_B \right), \tag{3.4.1}$$

$$\frac{\partial p_H}{\partial t} + v_H \frac{\partial p_H}{\partial x} + r_H c_H^2 \frac{\partial v_H}{\partial x} + \frac{2}{r_H} r_H c_H^2 v_{rH} = f_H \left(\frac{Q_H}{A_H} + r_H v_H F_H \right). \tag{3.4.2}$$

Integration of Eq. 2.3.5 over radial and angle coordinates for each of bundle and hole channel gives

$$\frac{\partial T_B}{\partial t} + v_B \frac{\partial T_B}{\partial x} + f_B T_B \frac{\partial v_B}{\partial x} - \frac{2 r_H}{r_B^2 - r_H^2} f_B T_B v_{rB} = \frac{1}{r_B C_{VB}} \left(\frac{Q_B}{A_B} + r_B v_B F_B \right), \tag{3.4.3}$$

$$\frac{\partial T_H}{\partial t} + v_H \frac{\partial T_H}{\partial x} + f_H T_H \frac{\partial v_H}{\partial x} + \frac{2}{r_H} f_H T_H v_{rH} = \frac{1}{r_H C_{VH}} \left(\frac{Q_H}{A_H} + r_H v_H F_H \right), \tag{3.4.4}$$

where: Q_B and Q_H represent the heat input/output in bundle and hole respectively, including the heat transfer between helium, strands and jacket. The last terms in the left sides of above 4 equations represent the energy exchange between the two channels. Q_B and Q_H can be expressed as:

$$Q_B = p_{hb}h_{hb}(T_H - T_B) + p_{stb}h_{stb}(T_{st} - T_B) + p_{jkb}h_{jkb}(T_{jk} - T_B), \tag{3.4.5}$$

$$Q_H = p_{hb}h_{hb}(T_B - T_H), \tag{3.4.6}$$

where: p_{hb} and h_{hb} are the wetted perimeter and heat transfer coefficient between hole and bundle, and so on.

Two additional energy balance equations for superconductor strands and cable jacket must be added for a completed set of equations:

$$A_{st}r_{st}C_{st}\frac{\partial T_{st}}{\partial t} - \frac{\partial}{\partial x}\left(A_{st}K_{st}\frac{\partial T_{st}}{\partial x}\right) = Q_{st}\ , \tag{3.4.7}$$

$$A_{jk}r_{jk}C_{jk}\frac{\partial T_{jk}}{\partial t} - \frac{\partial}{\partial x}\left(A_{jk}K_{jk}\frac{\partial T_{jk}}{\partial x}\right) = Q_{jk}\ . \tag{3.4.8}$$

where: Q_{st} and Q_{jk} represent the heat input/out in strands and jacket respectively, including AC loss and heat exchange between helium, strands and jacket. Q_{st} and Q_{jk} can be expressed as:

$$Q_{st} = Q_{st}^{ac} + p_{stb}h_{stb}(T_B - T_{st}) + p_{stjk}h_{stjk}(T_{jk} - T_{st}), \tag{3.4.9}$$

$$Q_{jk} = Q_{jk}^{ac} + Q_{jk}^{coup} + p_{stjk}h_{stjk}(T_{st} - T_{jk}) + p_{jkb}h_{jkb}(T_B - T_{jk}), \tag{3.4.10}$$

where: Q_{st}^{ac}, Q_{jk}^{ac}, and Q_{jk}^{coup} are AC loss in strand, AC loss in jacket and the 3D coupling heat transfer between adjacent cables respectively.

3.5 Summary of quasi-2D formulation

A set of equations for a quasi-2D model can be summarized as the following:

$$\frac{\partial v_B}{\partial t} + v_B\frac{\partial v_B}{\partial x} = -\frac{1}{r_B}\frac{\partial p_B}{\partial x} - 2f_B\frac{v_B|v_B|}{D_{hB}}\ , \tag{3.5.1}$$

$$\frac{\partial v_H}{\partial t} + v_H \frac{\partial v_H}{\partial x} = -\frac{1}{r_H}\frac{\partial p_H}{\partial x} - 2 f_H \frac{v_H |v_H|}{D_{hH}} \ , \tag{3.5.2}$$

$$r_B dr_{pB} \frac{\partial v_{rB}}{\partial t} + r_H dr_{pH} \frac{\partial v_{rH}}{\partial t} + r_B dr_{pB} v_B \frac{\partial v_{rB}}{\partial x} + r_H dr_{pH} v_H \frac{\partial v_{rH}}{\partial x}$$

$$+\left(r_H \frac{v_{rH}^2}{2} - r_B \frac{v_{rB}^2}{2} \right) = (1-k)(p_H - p_B) \ , \tag{3.5.3}$$

$$r_H v_{rH} = e_B r_B v_{rB} \ , \tag{3.2.6}$$

$$\begin{aligned} &\frac{\partial p_B}{\partial t} + v_B \frac{\partial p_B}{\partial x} + r_B {c_B}^2 \frac{\partial v_B}{\partial x} - \frac{2 r_H}{r_B^2 - r_H^2} r_B {c_B}^2 v_{rB} = 2 r_B f_B v_B f_B \frac{v_B |v_B|}{D_{hB}} \\ &+ \frac{f_B}{A_B} p_{hb} h_{hb} (T_H - T_B) + \frac{f_B}{A_B} p_{stb} h_{stb} (T_{st} - T_B) + \frac{f_B}{A_B} p_{jkb} h_{jkb} (T_{jk} - T_B) \end{aligned} \ , \tag{3.5.4}$$

$$\begin{aligned} &\frac{\partial p_H}{\partial t} + v_H \frac{\partial p_H}{\partial x} + r_H {c_H}^2 \frac{\partial v_H}{\partial x} + \frac{2}{r_H} r_H {c_H}^2 v_{rH} = 2 r_H f_H v_H f_H \frac{v_H |v_H|}{D_{hH}} \\ &+ \frac{f_H}{A_H} p_{hb} h_{hb} (T_B - T_H) \end{aligned} \ , \tag{3.5.5}$$

$$\begin{aligned} &r_B A_B C_{VB} \frac{\partial T_B}{\partial t} + r_B A_B C_{VB} v_B \frac{\partial T_B}{\partial x} + r_B A_B C_{VB} f_B T_B \frac{\partial v_B}{\partial x} - r_B A_B C_{VB} \frac{2 r_H}{r_B^2 - r_H^2} f_B T_B v_{rB} \\ &= r_B A_B v_B \cdot 2 f_B \frac{v_B |v_B|}{D_{hB}} + p_{hb} h_{hb} (T_H - T_B) + p_{stb} h_{stb} (T_{st} - T_B) + p_{jkb} h_{jkb} (T_{jk} - T_B) \end{aligned} \tag{3.5.6}$$

$$\begin{aligned} &r_H A_H C_{VH} \frac{\partial T_H}{\partial t} + r_H A_H C_{VH} v_H \frac{\partial T_H}{\partial x} + r_H A_H C_{VH} f_H T_H \frac{\partial v_H}{\partial x} + r_H A_H C_{VH} \frac{2}{r_H} f_H T_H v_{rH} \\ &= r_H A_H v_H \cdot 2 f_H \frac{v_H |v_H|}{D_{hH}} + p_{hb} h_{hb} (T_B - T_H) \end{aligned} \tag{3.5.7}$$

$$A_{st} r_{st} C_{st} \frac{\partial T_{st}}{\partial t} - \frac{\partial}{\partial x}\left(A_{st} K_{st} \frac{\partial T_{st}}{\partial x} \right) = Q_{st}^{ac} + p_{stb} h_{stb} (T_B - T_{st}) + p_{stjk} h_{stjk} (T_{jk} - T_{st}) \ , \tag{3.5.8}$$

$$A_{jk} r_{jk} C_{jk} \frac{\partial T_{jk}}{\partial t} - \frac{\partial}{\partial x}\left(A_{jk} K_{jk} \frac{\partial T_{jk}}{\partial x} \right) = Q_{jk}^{ac} + Q_{jk}^{coup} + p_{stjk} h_{stjk} (T_{st} - T_{jk}) + p_{jkb} h_{jkb} (T_B - T_{jk}) \ . \tag{3.5.9}$$

4. Example and results

A new code "Solxport3d.for" has been developed based on the above equations by updating existing codes: "TOKSCPF.FOR" and "SAITOKPF.FOR". Using CSIC as an example, a current pulse is applied in the insert coil from around 20 to 40 seconds. The resulted AC loss has peak values in the same time period. Figs. 4.1 to 4.5 show that all the results including temperatures, velocities, pressures, and densities agree well with the expectation.

The pressure for both bundle and hole is almost identical as expected because a fast mass, momentum and energy exchange between two channels by the radial helium velocity. The temperature difference between two channels are relatively large. The superconductor strands have the highest temperature and the helium in hole has the lowest temperature. The radial velocity is very small on the order of 10^{-6} m/s. Its distribution as a function of time and along the x axis well agrees with the temperature behavior in two channels. In the peak period of the applied current pulse, helium flows from the bundle to hole driven by the tiny pressure difference between the two channels.

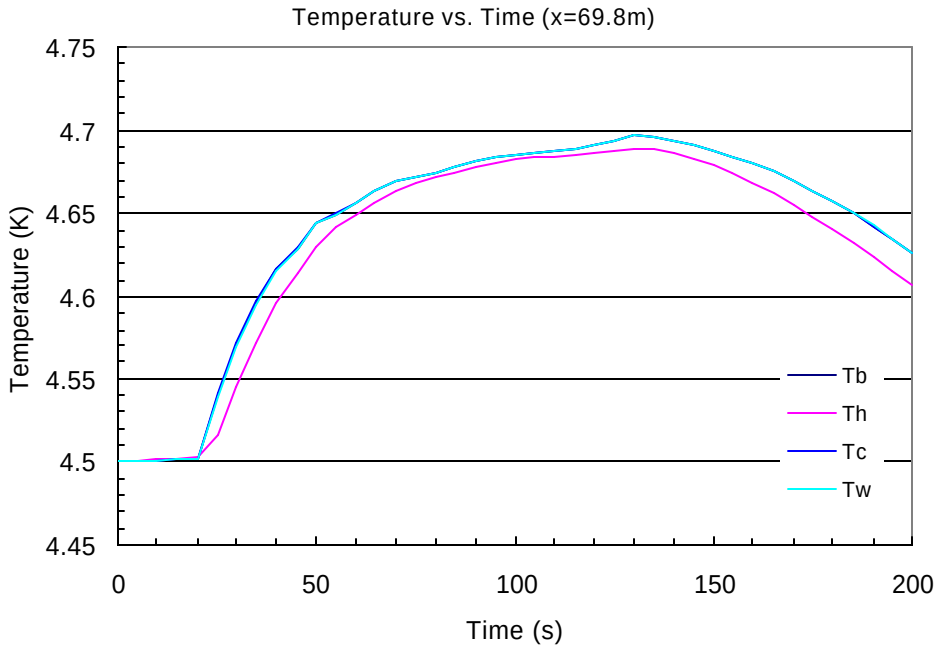

Fig. 4.1a Temperatures vs. time at x=69.8m (Tb: bundle helium temperature, Th: hole helium temperature, Tc: strands temperature, Tw: jacket temperature)

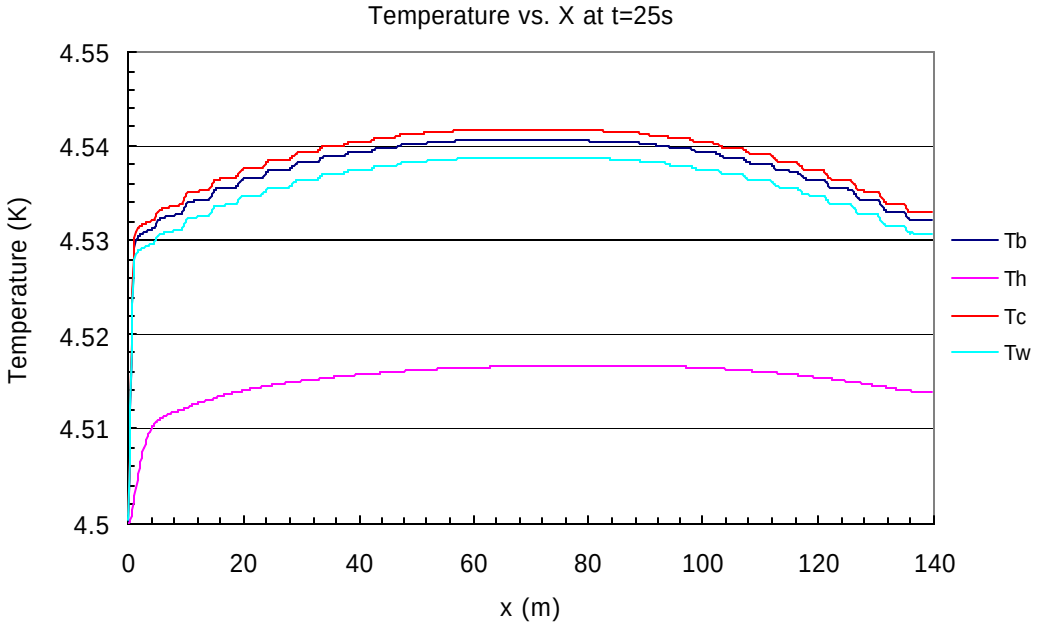

Fig. 4.1b Temperatures vs. x at t=25second. As expected, the strands have the highest temperature, the helium at hole has the lowest.

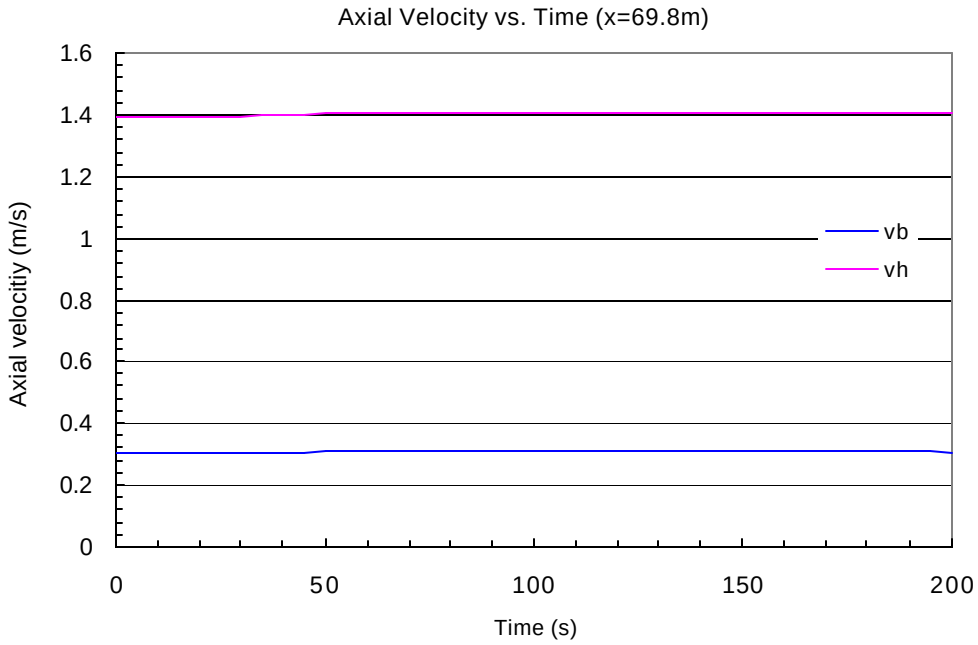

Fig. 4.2a axial velocity vs. time at x=69.8m (vb: helium velocity at bundle, vh: helium velocity at hole).

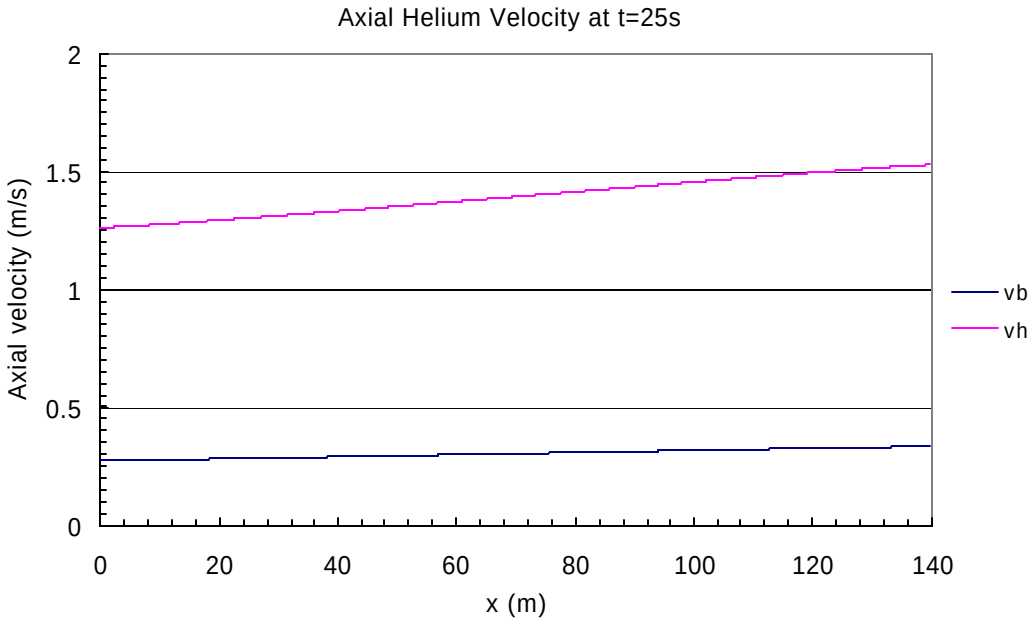

Fig. 4.2b Axial velocity vs. x at t=25second.

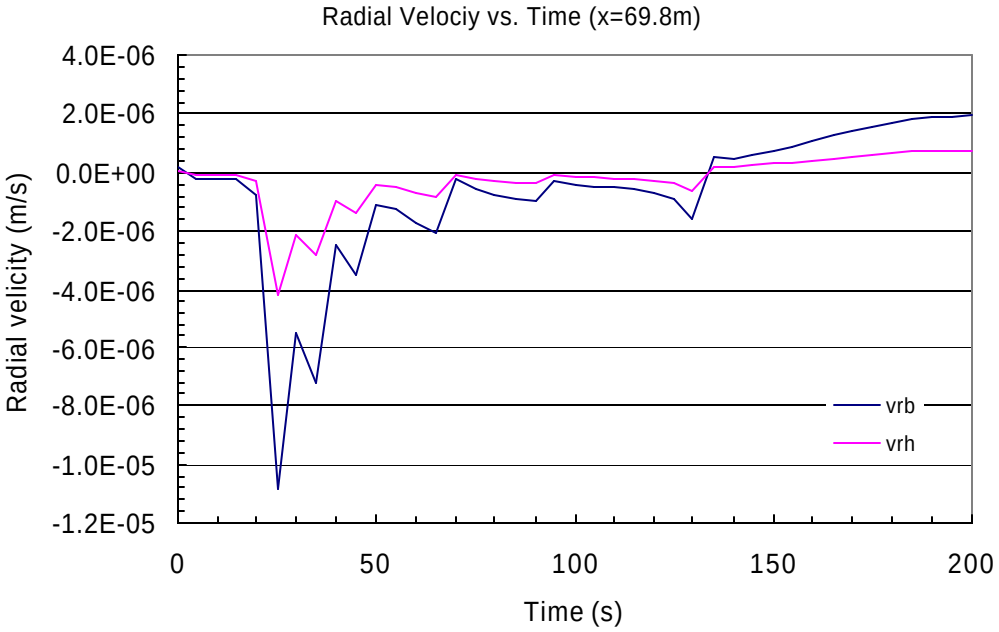

Fig. 4.3a Radial helium velocity vs. time at x=69.8m (vrb: radial velocity at bundle, vrh: radial velocity at hole), the negative values at the peak of applied current change indicate a helium flow from bundle to hole, which is expected as the helium temperature at bundle is higher than at hole.

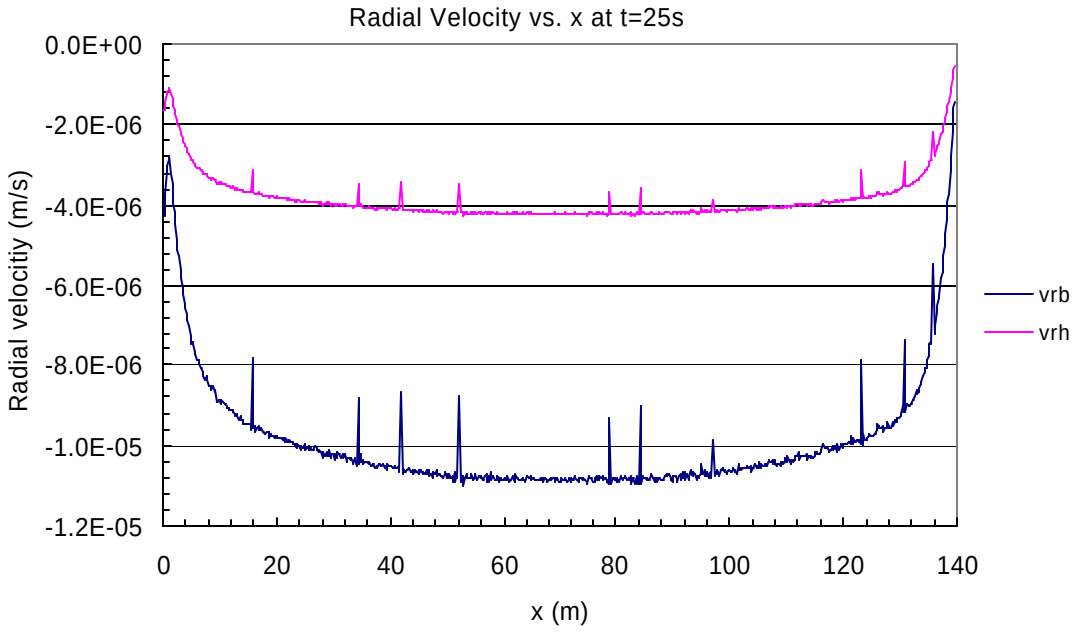

Fig. 4.3b Radial helium velocity vs. x at t=25second. The distribution curves of the radial velocity agree well with those of temperatures.

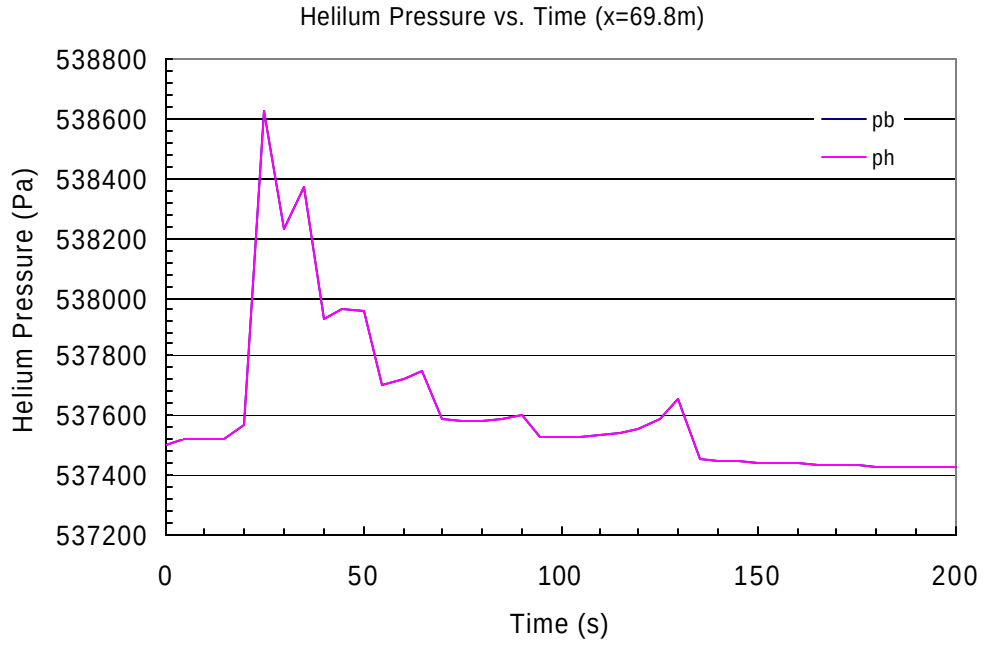

Fig. 4.4a Helium pressures vs. time at x=69.8m. The pressures at bundle and hole are almost overlapped.

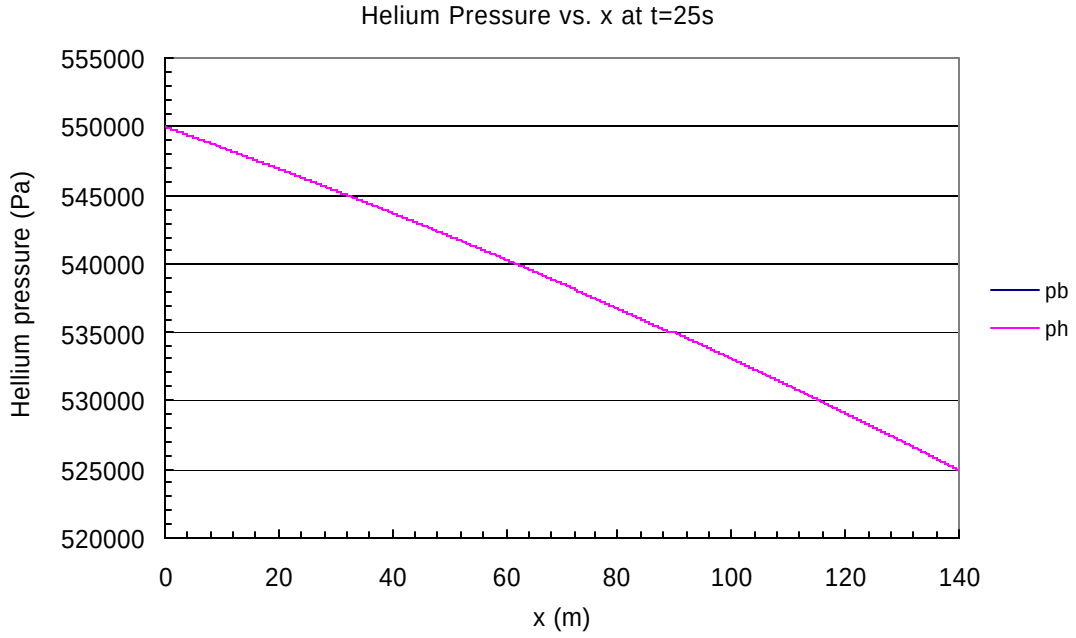

Fig. 4.4b Helium pressure vs. x at t=25second. Both pressures at bundle and hole are almost overlapped.

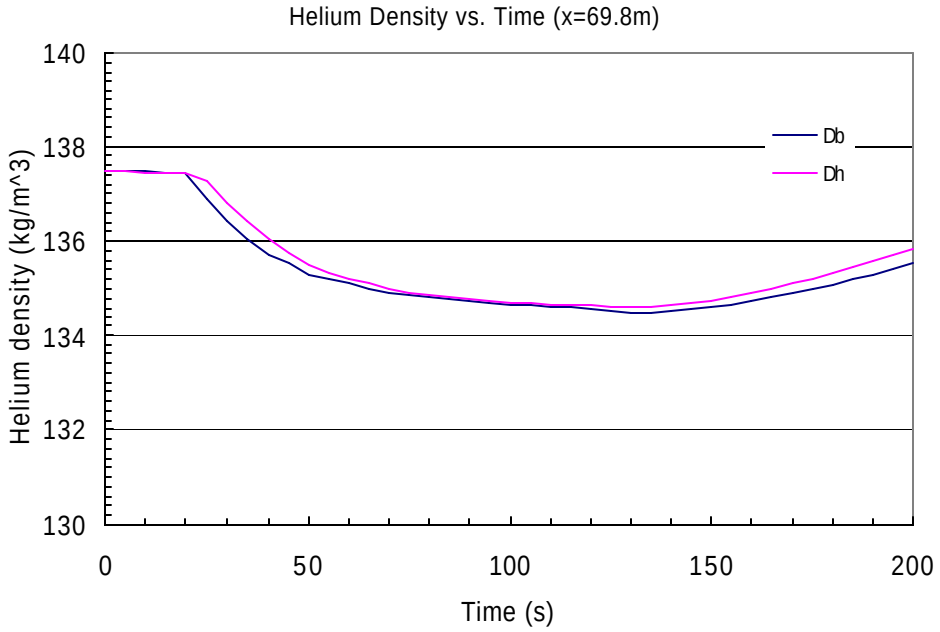

Fig. 4.5a Helium density vs. time at x=69.8m (Db: density at bundle, Dh: density at hole)

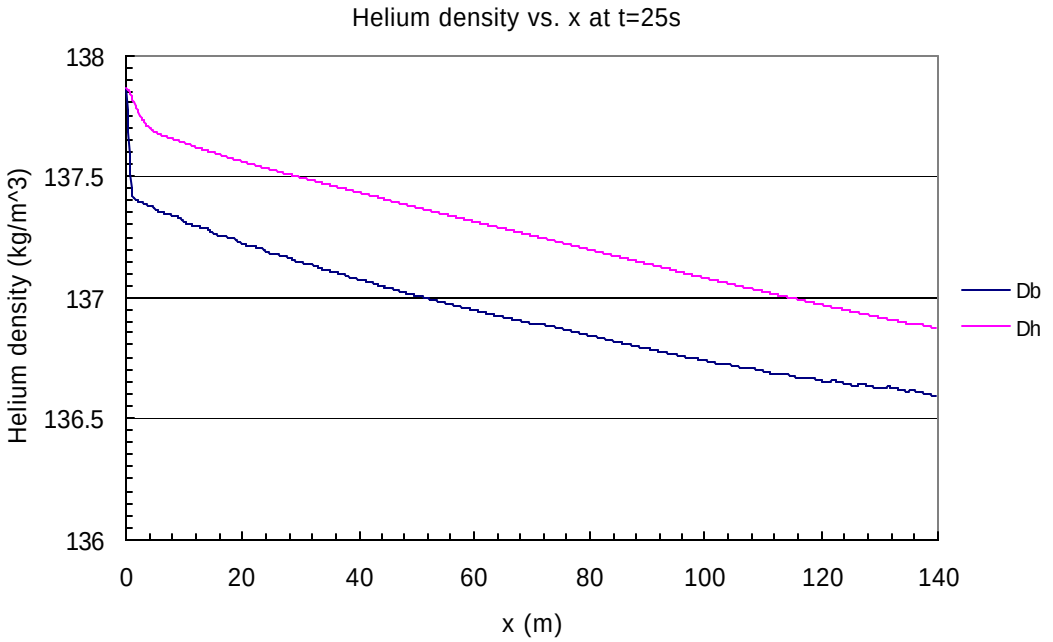

Fig. 4.5b Helium density vs. x at t=25second.

5. Calibration

The code and the simulation data have been calibrated based on mass and energy balance by using the above example. The following sections will report the results.

5.1 Mass balance calibration

Integration of the general mass balance equation 2.1.1 over the system gives the system mass balance equation:

$$\dot{m}_{inlet} - \dot{m}_{outlet} = \int_0^L \dot{r} \cdot A dx, \tag{5.1.1}$$

where: $\dot{m}_{inlet}$, $\dot{m}_{outlet}$ (kg/s) are mass flow rates at the inlet and outlet respectively. The left side of Eq. 5.1.1 is the difference of mass flow rate between the inlet and the outlet, and the right side is the mass accumulation in this system per second.

The error Δ (kg/s) and relative error $relative\Delta$ are defined respectively as:

$$\Delta = (\dot{m}_{inlet} - \dot{m}_{outlet}) - \int_0^L \dot{r} \cdot A dx \tag{5.1.2}$$

$$relative\Delta = \left| \frac{\Delta}{0.5(\dot{m}_{inlet} + \dot{m}_{outlet})} \right| \tag{5.1.3}$$

The results based on the above example are shown in Figs 5.1.1 and 5.1.2. The obtained relative mass balance error is less than 2.8%. The maximum error appears at the peak of applied current change. This simulation uses 700 elements with time step of 0.05 second. The error could be improved if refining the space mesh and time step. The first order approximation of Eq. 3.2.6 may also contribute to these errors.

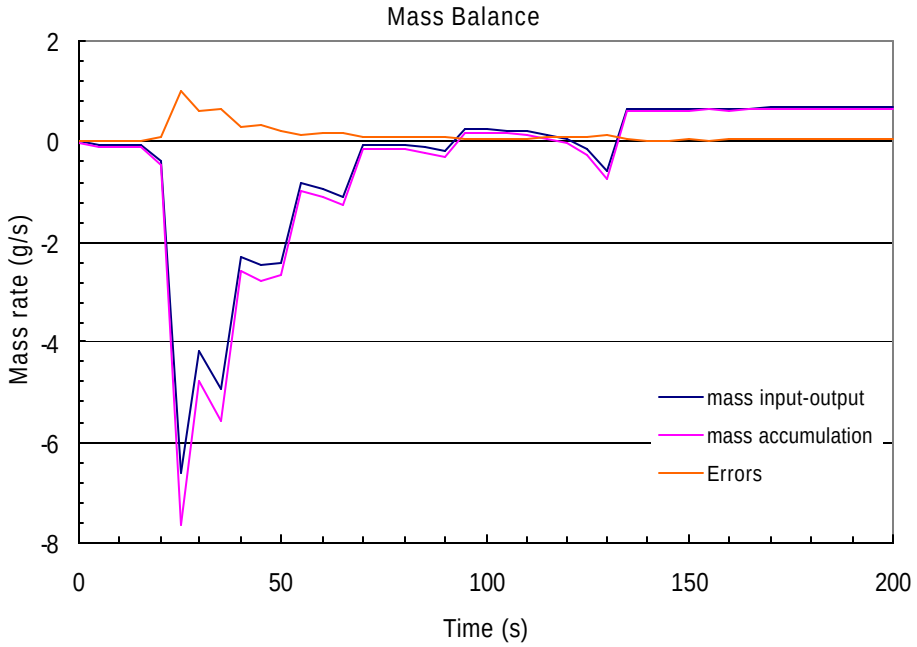

Fig. 5.1.1 Mass balance results based on Eq. 5.1.2 (time step =0.05s).

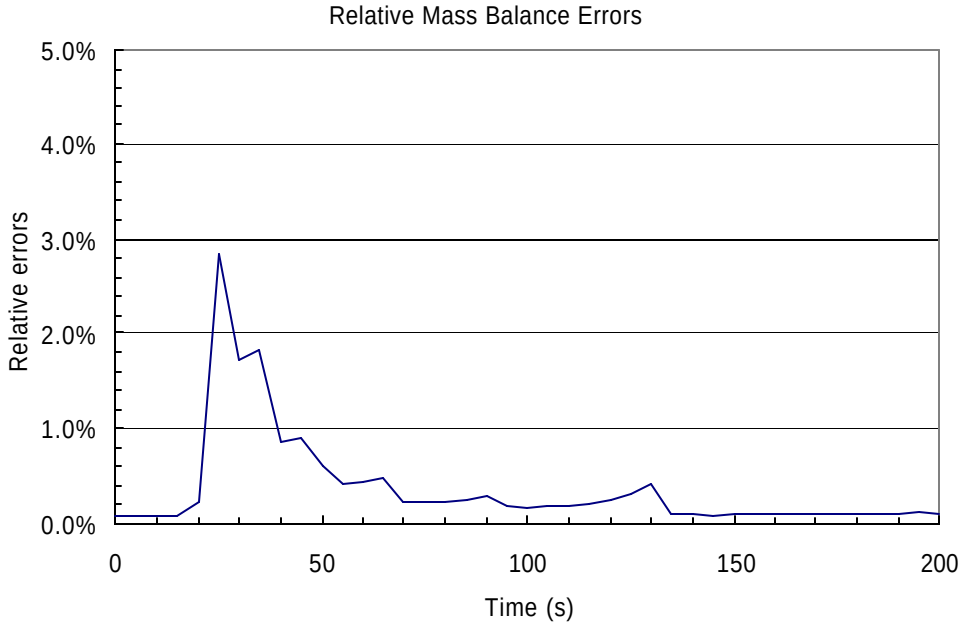

Fig. 5.1.2 Relative mass balance errors vs. time. The maximum relative error of 2.8% appears at the peak of applied current change.

5.2 Energy balance calibration

Integration of the general energy balance equation 2.2.9 over the system gives the system energy balance equation:

$$\begin{aligned}
&\sum\left(A_c r_c C_c \frac{\partial T_c}{\partial t} + A_w r_w C_w \frac{\partial T_w}{\partial t} + A_b r_b C_b \frac{\partial T_b}{\partial t} + A_h r_h C_h \frac{\partial T_h}{\partial t}\right)\Delta x \\
&+ \sum (A_b r_b C_b v_b) T_b \Big|_x^{x+\Delta x} + \sum (A_h r_h C_h v_h) T_h \Big|_x^{x+\Delta x} \\
&+ \sum (A_b r_b C_b f_b T_b) v_b \Big|_x^{x+\Delta x} + \sum (A_h r_h C_h f_h T_h) v_h \Big|_x^{x+\Delta x} \\
&+ \sum 2\pi r_h \left(r_h C_h f_h T_h v_{rh} - r_b C_b e_b f_b T_b v_{rb}\right)\Delta x \\
&= \left(A_c K_c \frac{\partial T_c}{\partial x}\right)_{inlet}^{outlet} + \left(A_w K_w \frac{\partial T_w}{\partial x}\right)_{inlet}^{outlet} \\
&+ \sum (A_b r_b v_b F_b + A_h r_h v_h F_h)\Delta x \qquad (5.2.1) \\
&+ \sum \left(Q_c^{ac} + Q_w^{ac}\right)\Delta x
\end{aligned}$$

where: A_c, A_w, A_b, A_h (m^2) are cross sections; r_c, r_w, r_b, r_h (kg/m^3) are densities; C_c, C_w, C_b, C_h (J/kg-K) are specific heat; $K_{c,} K_w$ (W/m-K) are thermal conductivity; Q_c^{ac}, Q_w^{ac} (W/m) are AC losses. The subscripts c, w, b, h represent conductor, wall, helium in bundle and helium in hole respectively.

The 1st term of the left side represents energy increase due to rising temperature. The 2nd to 5th terms of the left side represent the effect due to axial convection. The last term of the left side represents the effect due to radial convection. The first 2 terms of the right side represent the thermal conduction at inlet and outlet, and they are neglected in the current model. The third term of the right side represents the friction effect. The last term of the right side represents the AC loss. The 3D coupling heat exchange between adjacent cables is not considered in this example.

The errors Δ of energy balance is defined as the differences between both sides of the Eq. 5.2.1:

$$\Delta = left\_side - right\_side . \qquad (5.2.2)$$

The relative error is defined as the ratio of the errors against the inputted energy (AC loss + friction term):

$$relative\Delta = \left| \frac{\Delta}{\sum (A_b r_b v_b F_b + A_h r_h v_h F_h)\Delta x + \sum \left(Q_c^{ac} + Q_w^{ac}\right)\Delta x} \right| . \qquad (5.2.3)$$

The results based on the above example are shown in Figs. 5.2.1 and 5.2.2 The relative errors of the energy balance are less than 1.3%. It also could be improved by refining the space mesh and time step. Further work is needed.

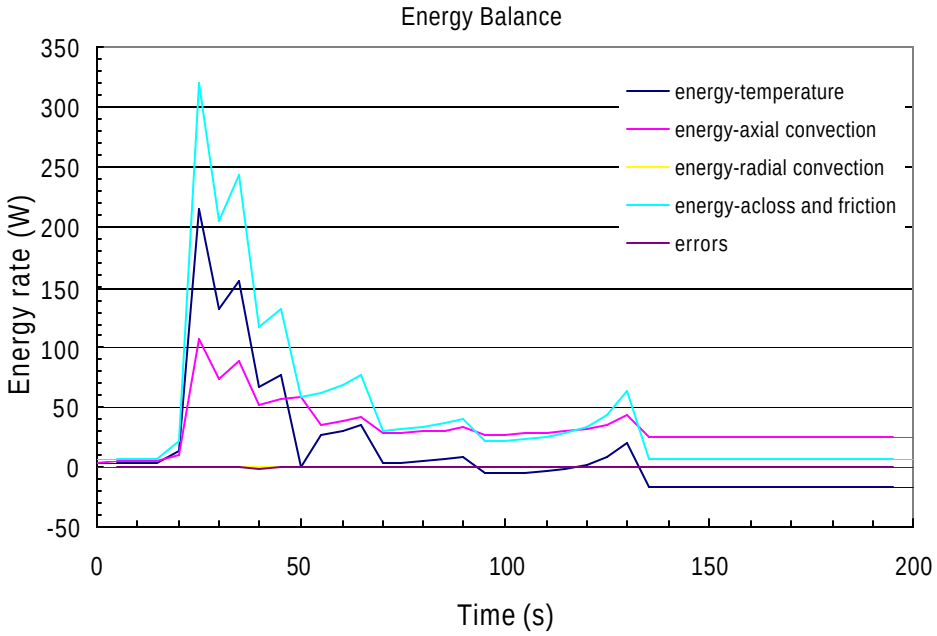

Fig. 5.2.1 Energy balance results, showing that energy term with radial convection is very small and the errors are very small (time step =0.05s).

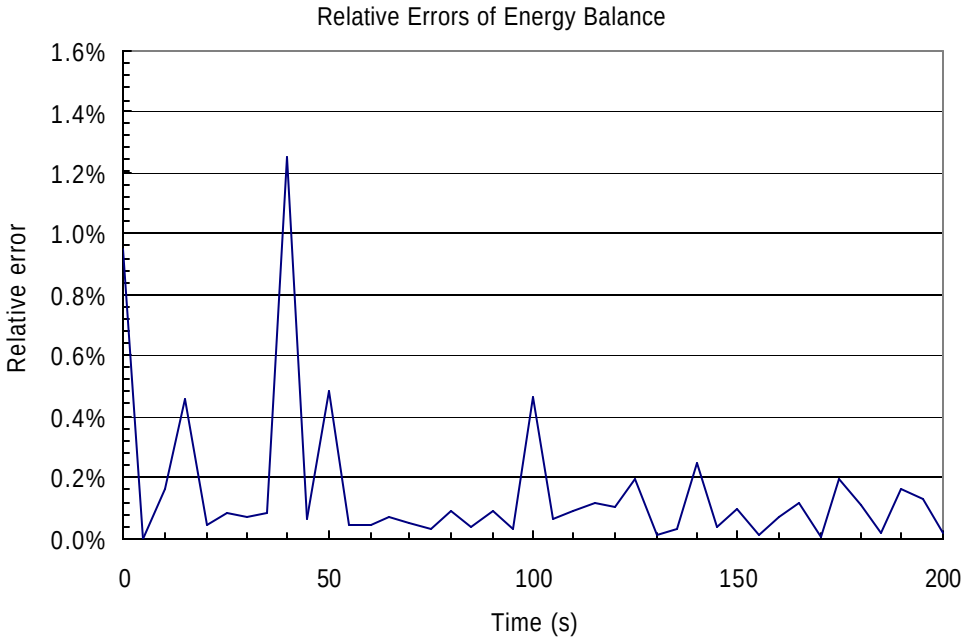

Fig. 5.2.2 The relative energy balance errors vs. time. The maximum relative error is less than 1.3%.

6. Conclusions

A quasi-2D model has been developed. The results agree well with the expectations. The pressure difference between the two channels is very small. It is due to fast mass, momentum and energy exchange between the two channels. The temperature difference between the two channels is relatively larger. It is interesting to see that the variation of radial helium velocity between the two channels is consistent with those temperatures. The radial velocity is very small on the order of 10^{-6} m/s, but plays a very important role in pressure balance and energy transfer between the two channels.

The relative errors for mass and energy are less than 2.8% and 1.3% respectively, indicating an acceptable accuracy of the calculated results. These errors could be improved if refining space mesh and time step.

Acknowledgements

The author would like to thank the colleagues in PSFC of MIT for valuable discussions. This work was supported by the US Department of Energy under Grant DE-FC02-93ER54186.

References

[1] Bottura L., A numerical model for the simulation of quench in the ITER magnets, J. Comput Phys, Vol. 125, 1996, pp. 26-41.

[2] Zanino R., Palo S. De, and Bottura L., A Two-Fluid Code for the Thermohydraulic Transient Analysis of CICC Superconducting Magnets, J. Fusion Energy, Vol. 14, No. 1, 1995, pp. 25-40.

[3] Shajii A. Theory and Modeling of Quench in Cable-In-Conduit Superconducting Magnets, Ph. D. thesis, MIT, 1994.

[4] Bird, R.B., Stewart, W.E., Lightfoot, E.N., Transport Phenomena, pub. by John Wiley&Son, 1960.

[5] Hildebrand F.B., Advanced Calculus for Applications, pub. by Prentice-Hall, 1976.